*Monografías de la Real Academia de Ciencias de Zaragoza* **32**, 39–63, (2009).

# Effect of primordial size distributions on the formation of Kuiper-belt binaries

David Farrelly

Departamento de Química C–IX

Universidad Autónoma de Madrid, Cantoblanco, 28049 Madrid

and

Department of Chemistry,

Utah State University, Logan, UT 84322-0300, U.S.A.

**Abstract**

Near-symmetric binaries - i.e., binaries with roughly same-sized partners - appear to dominate the known population of binaries in the Kuiper-belt. Herein the mass- and size-ratio distributions of Kuiper-belt binaries predicted by the chaos-assisted capture formation model are investigated. The basic proposition is that capture requires that two objects, initially following heliocentric Keplerian orbits, must enter their mutual Hill sphere before binary formation becomes possible. Simulations in the Hill problem demonstrate that a window of relative asymptotic velocities exists outside of which Hill sphere entry is unlikely. On the other hand, equipartition arguments, as well as coagulation calculations, suggest that a given body's velocity will depend on its mass. This, in turn, establishes a link between the mass - or size (diameter) - of a body and the feasibility of it being captured into a binary. Larger bodies moving with velocities roughly comparable to the Hill velocity are most likely to fall within the capture window. Stabilization is then possible through gravitational scattering with smaller, faster-moving intruders. Uniform and power-law initial mass and size distributions are used to study this scenario in the four-body Hill approximation. A velocity-size relationship similar to that obtained from coagulation calculations but augmented with a gaussian spread is used. The contribution and role of exchange reactions is also investigated. Selection for roughly same-sized binary partners is found to arise partly from (i) the capture window that selects for Hill sphere entry and partly from (ii) the preference for near-symmetric binaries to be stabilized by gravitational scattering with intruders.

## 1 Introduction

The trans-Neptunian part of the Solar System - the Edgeworth-Kuiper-belt or just "the Kuiper-belt" - is a unique laboratory for testing planetary formation models (Kenyon, 2002; Lykawa and Mukai, 2005; Noll et al., 2007). This is because this region is thought to consist of leftovers from the accretional phase of the Solar System (Stern, 1996; Kenyon and Luu, 1998). Consequently, trans-Neptunian objects (TNOs) potentially provide a window into the earliest epochs of the Solar System. Ideally, one would like to understand how the Kuiper-belt evolved to its present state, how (and if) orbital and spectral properties correlate with each other (Barucci et al., 2001; Cruikshank, 2003, 2005), the physical structure of TNOs; and the relationship between TNOs and other objects in the Solar System - e.g., is Triton a captured TNO? (McKinnon and Leith, 1995; Cruikshank, 2005; Agnor and Hamilton, 2006). Because of their remoteness, however, knowledge of the dynamical, physical, and chemical properties of TNOs remains quite limited. Nevertheless, progress on all these fronts is being made through the recent discovery of a significant population of binary TNOs (Noll, 2003, 2006; Brown et al., 2006; Stephens and Noll, 2006; Noll et al., 2007).

Binaries are important in all areas of astronomy because they provide a direct way of determining the total mass of the system under study; this information then paves the way for determining other system properties that can, in their turn, be used to shed light on the formation and dynamical evolution not only of the binary itself, but possibly of other objects in its locale (Noll, 2006). For example, knowledge of the mass-ratio distributions of stellar binaries provides a way to discriminate between different formation scenarios. Broadly speaking, stellar binary formation models can be categorized either as "matchmaking" or as "birth" models (Bonnell, 2001; Goldberg et al., 2003). In matchmaking models it is assumed that the two stars were formed separately and only later came together in a binary. On the other hand, birth models assume that the two stars were formed together. An analogy exists in the Solar System: The regular moons of Jupiter and Saturn are thought to have been formed alongside their parent planet while their irregular satellites (and Triton at Neptune) are thought to have been captured (McKinnon and Leith, 1995; Agnor and Hamilton, 2006). In the case of Solar System binaries, a third channel - physical collisions - must be added to the list of possible binary formation mechanisms (Stern, 1995).

Kuiper-belt binaries (KBBs) are of special interest because they have unusual physical and orbital properties, at least when compared to the properties of near-Earth and main-belt asteroid binaries. For example, KBBs tend to have partner mass-ratios of order unity whereas other Solar System asteroid binaries typically have mass ratios in the range $m_r \sim 10^{-3} - 10^{-4}$ where $m_r = m_2/m_1$ and $m_1$ and $m_2$ are the masses of the binary partners with

$m_2 \leq m_1$ (Durda et al., 2004a). Orbital peculiarities include large mutual orbit semi-major axes ($a$) compared to the physical radii ($r_1$, $r_2$) of the binary components themselves and moderately large eccentricities (Noll, 2003; Noll et al., 2007). The bracketing of different KBB properties is useful because it provides constraints on Solar System formation models as well as KBB formation models.

A caveat is in order: Because Kuiper-belt objects (KBOs) are so remote and faint, any apparent preference for near-symmetric binaries (and large semi-major axes) might simply be the result of observational bias. For example, it might be easier to detect binaries in the first place because two objects in a binary will typically appear brighter than either one separately. The first KBB to be discovered (1998 $WW_{31}$), in fact, was not immediately recognized to be a binary (Veillet et al., 2002). Furthermore, if $m_1$ and $m_2$ are similar in size and albedo, and are sufficiently well separated, then the object will be more easily recognized to be a binary than if, say, $m_1 \gg m_2$. Other sources of uncertainties must also be considered. The brightness of a TNO is a function of its diameter and albedo and, therefore, mass comparisons between objects based only on visual magnitudes must necessarily make assumptions about the albedos and densities of the binary partners. While assuming similar densities and albedos is probably reasonable, it is worth noting that the albedoes and densities of Pluto and Charon are quite different from each other (Reinsch et al., 1994; Person et al., 2006). In principle, individual masses can be determined more directly (e.g., from observations of occultations) although few if any such measurements have so far been made of KBBs. Despite these uncertainties, based on observations using the Hubble Space Telescope, Noll et al. (2006, 2007), have concluded that the apparent preference for near-symmetric KBBs may be real. This has significant implications for models of their formation.

In principle, different binary formation mechanisms will produce different mass-ratio distributions. Computed distributions will also depend on assumptions made about the primordial mass and velocity distributions of KBOs. For example, in dynamical capture scenarios, the simplest model might be to pair KBOs at random from some assumed initial KBO mass distribution. In this case the mass distributions of $m_1$ and $m_2$ in the binary ought to be independent of each other. However, it is unlikely that binary formation is completely random. Indeed, studies of stellar binary formation in the three-body problem indicate that, for example, in star clusters exchange reactions tend to produce roughly same-sized binary partners, i.e., near-symmetric binaries (Hills, 1990; Heggie and Hut, 2003; Funato et al., 2004). Another possibility is that binaries of particular mass-ratios are more robust to perturbations. Thus, dynamical effects need to be to considered as a factor that determines the mass-ratio distribution of KBBs (Valtonen and Mikkola, 1991; Valtonen, 1998).

In the recently proposed chaos-assisted capture (CAC) (Astakhov et al., 2003) scenario

of binary formation, two potential binary partners may become trapped for long periods of time inside chaotic layers within their mutual Hill sphere (Astakhov et al., 2005; Lee et al., 2007). The binary is then captured permanently through gravitational scattering with a third "intruder" body. The creation of binaries having similarly sized partners is an *ab initio* prediction of the model. Recently, Iwasaki and Ohtsuki (2007) have emphasized the possible role of long-term temporary trapping inside the Hill sphere in the capture of irregular moons and the formation of KBBs.

The main objective of the paper is to test whether the CAC mechanism - and in particular, its prediction of a preference for near-symmetric binaries (Astakhov et al., 2005; Lee et al., 2007) - can survive the incorporation of more realistic mass and velocity distributions than the uniform distributions used previously, e.g., by Lee et al. (2007). It turns out that the dynamical mechanism by which CAC selects for binaries having mass-ratios in the range $m_2/m_1 \sim 0.1 - 1$ (i.e., near-symmetric binaries) is augmented by a second mechanism. This mechanism relates to the initial entry into the Hill sphere and is found to occur through a velocity window that, in turn, acts as a selector for mass.

This paper is organized as follows: Section 2 provides a brief overview of current KBB formation models. The algorithm used is described in Sec. 3, and the results obtained for uniform mass-ratio and power-law size-ratio distributions are presented in Sec. 4. Conclusions are in Sec. 5, together with a brief discussion of the possible relevance of the CAC mechanism to binary formation in the Asteroid Belt.

## 2 Overview of Kuiper-belt binary formation models

A number of models have been proposed to explain how KBBs formed (Weidenschilling, 2002; Goldreich et al., 2002; Funato et al., 2004; Astakhov et al., 2005; Lee et al., 2007), and several discussions of the various binary formation models exist in the literature (Weidenschilling et al., 1989; Merline et al., 2002; Noll, 2006; Noll et al., 2007; Kern and Elliot, 2006; Cruikshank et al., 2006). Formation models can be broken down into two broad categories: those involving physical collisions and those that rely on dynamical processes (e.g., gravitational scattering.) The physical and orbital properties of KBBs seem to rule out physical collisions as a major contributing pathway. In particular, KBBs appear to have too much orbital angular momentum to have been formed directly through collisions (Margot, 2002; Burns, 2004; Durda et al., 2004a; Stern, 2002; Canup, 2005; Chiang et al., 2006). Their relatively large semi-major axes and large mass-ratios also argue against this formation channel. Setting physical collisions aside leaves dynamical models of the "matchmaking" variety. These models must (i) explain how two bodies that come close to each other can lose enough energy for capture to become permanent, and (ii) they must account for the observed compositional and orbital properties of KBBs,

namely, large, moderately eccentric orbits and nearly same-sized partners.

The various dynamical processes and outcomes may be summarized as follows:

$$\{m_1, m_2\}^* + m_3 \rightarrow \{m_1, m_2\} + m_3^* \qquad \text{direct stabilization} \tag{1a}$$

$$\{m_1, m_2\}^* + m_3 \rightarrow \{m_1, m_3\} + m_2^* \qquad \text{exchange stabilization} \tag{1b}$$

$$\{m_1, m_2\}^* + m_3 \rightarrow m_1^\dagger + m_2^\dagger + m_3^\dagger \qquad \text{ionization} \tag{1c}$$

where $\{m_1, m_2\}$ indicates a binary consisting of $m_1$ and $m_2$; the "*" denotes excess energy that must be extracted in order for a stable binary to result; the "†" symbol indicates that the binary energy is distributed, not necessarily equally, between the fragments.

## 3 Capture inside the Hill sphere

Details of the basic CAC model are available elsewhere (Astakhov et al., 2003, 2005; Lee et al., 2007).

The capture dynamics takes place inside the Hill sphere, i.e., the region of space lying between the Lagrange points $L_1$ and $L_2$ in Hill's problem and of radius

$$R_H = a_\odot \left( \frac{m_1 + m_2}{3M_\odot} \right)^{\frac{1}{3}} \tag{2}$$

where $M_\odot = m_0$ is the mass of the Sun (Murray and Dermott, 1999). Particles entering the Hill sphere, in the main, either enter chaotic layers or scatter out of the Hill sphere promptly (Simó and Stuchi, 2000; Astakhov et al., 2003; Astakhov and Farrelly, 2004; Astakhov et al., 2005). Those binaries that happen to enter chaotic layers may survive for many heliocentric orbital periods (at 45 AU the heliocentric orbital period, $T \sim 300$ years) whereas chaotic transient or quasi-binary orbits can remain trapped inside the Hill sphere for $\sim 10^3 - 10^5$ years or longer - see Fig. 1 (Lee et al., 2007). After the quasi-binary has formed, it can then be stabilized by, in principle, a variety of external perturbations that succeed in pushing the chaotic orbit into an adjacent (in phase space) regular region. In the CAC model of KBB binary formation, it is assumed that gravitational scattering with a series of intruder particles leads to stabilization and orbit reduction although this is not the only possible stabilization mechanism (Astakhov et al., 2005; Lee et al., 2007).

All of the calculations are performed in either the three- or the four-body Hill approximations.

### *3.1 Four-body Hill problem*

The Hill four-body problem is the generalization of the usual three-body Hill problem, which it contains as a special case. The basic assumption is that three small bodies, with a mutual center-of-mass, $\mathbf{R}_c$, orbit a much larger fourth body (the Sun, $m_0 = 1$) on

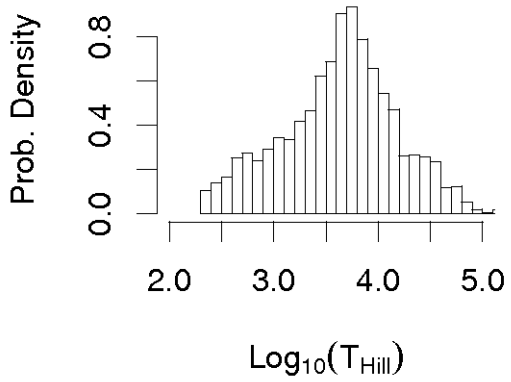


Figure 1.— Histogram showing $\log_{10}$ of the Hill lifetimes ($T_{Hill}$) in years for the cohort of chaotic quasi-binaries used in the simulations and which actually are captured. The Hill lifetime is defined to be the total time that a given trajectory, corresponding to a set of binary initial conditions launched from infinity, would remain within the Hill sphere in the three-body Hill approximation, i.e., in the absence of intruder scattering, for example. At 45 AU the orbital period is $\sim 300$ years $\equiv 2\pi$ in dimensionless Hill units at 45 AU. Conversion between physical units (years) and Hill units requires knowledge of the distance to the Sun.

a nearly circular orbit (*e.g.*, three small Kuiper-belt objects interacting gravitationally). The generalization of the three-body Hill problem is due to Scheeres (1998). Assume that the total mass of the three small bodies is given by

$$\mu = \sum_{j=1}^{3} m_j \ll 1. \tag{3}$$

Setting $\mathbf{R}_c \simeq \mathbf{a} = (1, 0, 0)$ defines the motion of the three-body center-of-mass along an almost circular orbit that defines the rotating frame. The vector equations of motion are (Scheeres, 1998)

$$\ddot{\boldsymbol{\rho}}_i + \boldsymbol{\Omega} \times [2\dot{\boldsymbol{\rho}}_i + \boldsymbol{\Omega} \times \boldsymbol{\rho}_i] = -\boldsymbol{\rho}_i + 3\mathbf{a}(\mathbf{a} \cdot \boldsymbol{\rho}_i) + \sum_{k=1}^{3}{}' \alpha_k \frac{\boldsymbol{\rho}_{ik}}{|\boldsymbol{\rho}_{ik}|^3}, \qquad i = 1, 2, 3 \tag{4}$$

where $\boldsymbol{\rho}_{ik} = \boldsymbol{\rho}_k - \boldsymbol{\rho}_i$ and the summation convention $\sum'$ means that terms with $i = k$ are excluded. The $\alpha_k$ are defined through $m_j = \mu\alpha_j$ where

$$\sum_{j=1}^{3} \alpha_j = 1 \tag{5}$$

and the coordinates $\boldsymbol{\rho}_1, \boldsymbol{\rho}_2, \boldsymbol{\rho}_3$ are related through the center-of-mass relation

$$\sum_{j=1}^{3} \alpha_j \boldsymbol{\rho}_j = 0. \tag{6}$$

If $\alpha_3 = 0$, then the problem reduces to the Hill three-body problem for $m_1$ and $m_2$. In this limit the problem can also be thought of as the restricted Hill four-body problem for the mass-less test-particle, $m_3$.

In some simulations the elliptical three-body Hill problem (EHP) will be used. The EHP contains the three-body circular Hill problem (CHP) as a special case. Setting $m_1 + m_2 = \nu$ with $\nu \ll m_0 = 1$ (using the slightly non-standard definitions of Scheeres (1998)) the Hamiltonian is the following (Szebehely, 1967; Ichtiaroglou, 1980; Moons et al., 1988; Llibre and Pinol, 1990; Brumberg and Ivanova, 1990; Astakhov and Farrelly, 2004; Astakhov et al., 2005; Palacian et al., 2006):

$$\begin{aligned} H = E = \frac{1}{2}(p_x^2 + p_y^2 + p_z^2) + \frac{1}{2}(x^2 + y^2 + z^2) - (x\,p_y - y\,p_x) \\ - \frac{1}{(1 + e_\odot \cos f_\odot)} \left( \frac{3x^2}{2} + \frac{1}{|\boldsymbol{\rho}|} \right) + \frac{81^{\frac{1}{3}}}{2} + O(\nu^{\frac{1}{3}}). \end{aligned} \tag{7}$$

Here $E$ is the energy, $(x, y, z) = \mathbf{r}$ defines the relative position of the binary members $m_1$ and $m_2$, and $(p_x, p_y, p_z) = \mathbf{p}$ is the corresponding momentum vector. The coordinate system $(x, y, z)$ is rotating with constant heliocentric angular frequency $\boldsymbol{\Omega}_\odot = (0, 0, 1)$ in the $x - y$ plane. The eccentricity and true anomaly of the heliocentric orbit of the binary barycenter are $e_\odot$ and $f_\odot$ respectively. In this coordinate system the barycenter of the two small bodies is located at the origin. The additive constant is chosen such that the Lagrange saddle points (Murray and Dermott, 1999) in the circular ($e_\odot = 0$) limit occur at $E = 0$.

### *3.2 Monte Carlo simulations*

Figure 4 provides a general overview of the approach taken. Apart from the selection of initial mass distributions, the approach is identical to that described by Lee et al. (2007).

### *3.3 Velocity window at infinity*

The two potential binary partners - the primaries - are initially assumed to be following heliocentric orbits with semi-major axes $a_1$ and $a_2$ with some velocity dispersion, $V$, around a Keplerian orbit lying in the invariant plane with semi-major axis $a_\odot$. The asymptotic orbital elements of the relative motion are (Hénon and Petit, 1986; Petit and

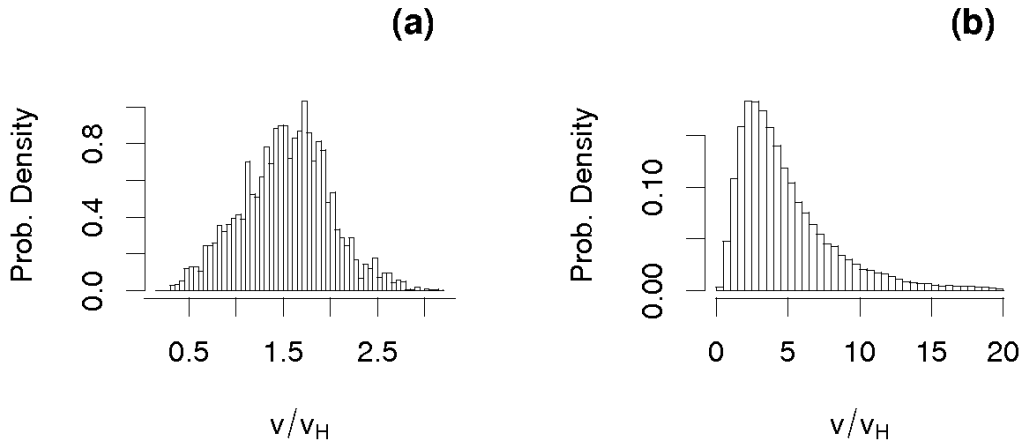


Figure 2.— Histograms showing the distributions of asymptotic random velocities, $v$, -see eq. (11) - which lead to penetration of the Hill sphere in (a) the circular and (b) the elliptic three-body problems. In (b) heliocentric eccentricties were chosen randomly in the range $e_\odot \in (0, 0.3)$. Velocities are scaled by the Hill velocity, $v_H$ - see eq. (10)

Hénon, 1986, 1987)

$$\begin{aligned} x &= a - e\,\cos(t-\tau) \\ y &= -\tfrac{3}{2}\,a\,(t-\phi) + 2\,e\,\sin(t-\tau) \\ z &= i\,\sin(t-\omega) \\ \dot{x} &= e\,\sin(t-\tau) \\ \dot{y} &= -\tfrac{3}{2}\,a + 2\,e\,\cos(t-\tau) \\ \dot{z} &= i\,\cos(t-\omega) \end{aligned} \tag{8}$$

where $a, e$, and $i$ are the Hill, or "reduced," orbital elements: Here $b = |a|$ is the impact parameter, $e$ is the eccentricity and $i$ is the inclination in Hill units while $\tau, \phi$, and $\omega$ are phase angles. Explicitly, the reduced elements are related to the semi-major axis ($a^*$), eccentricity ($e^*$) and inclination ($i^*$) in the circular restricted three-body problem as follows (Nakazawa and Ida, 1988; Nakazawa et al., 1989; Ohtsuki and Ida, 1990; Wetherill and Stewart, 1989; Greenzweig and Lissauer, 1990, 1992; Wetherill and Stewart, 1993).

$$\begin{aligned} a &= \frac{(a^* - a_\odot)}{R_H} \\ e &= \frac{a_\odot\, e^*}{R_H} \\ i &= \frac{a_\odot\,\sin(i^*)}{R_H} \end{aligned} \tag{9}$$

It is useful to scale velocities by the Hill velocity, $v_H$, which is the orbital velocity around a large body at the Hill sphere radius assuming no solar perturbations (Goldreich

et al., 2004; Rafikov, 2003; Murray-Clay and Chiang, 2006), i.e.,

$$V_H = \left[\frac{G(m_1 + m_2)}{R_H}\right]^{\frac{1}{2}} \sim \Omega_\odot \, R_H. \tag{10}$$

where $G$ is the gravitational constant and $\Omega_\odot$ is the heliocentric orbital frequency. In Hill units, the Hill velocity $v_H = 3^{-1/6} \sim 1.2$, or, in physical units, $V_H \sim 0.9$ m/s (lower case symbols will be used for velocities expressed in Hill units) at $a_\odot \sim 45$ AU. Conversion between physical and scaled velocities requires knowledge of $a_\odot$ and the mass of the binary.

At large separations the random component of the relative velocity is defined, in Hill units (Safronov, 1972; Weidenschilling, 1989; Greenzweig and Lissauer, 1990; Shiidsuka and Ida, 1999; Stern, 1995; Shiidsuka and Ida, 1999),

$$v_{\rm rand} = \frac{R_H}{a_\odot}\sqrt{e^2 + i^2}\, v_K \tag{11}$$

where $a_\odot$ is the heliocentric semi-major axis and $v_K$ is the local circular Keplerian velocity, also in dimensionless Hill units. The shear velocity is defined to be $v_{\rm shear} = |\frac{3}{2}a|$.

The random velocity has been used as a metric to distinguish the shear and dispersion dominated regimes, e.g., by comparing it to the Hill velocity. Various workers have employed slightly different definitions of the random velocity, e.g., Wetherill and Cox (1984) differ from Safronov (1972) and these differ from Greenzweig and Lissauer (1990). It is generally the random component of the asymptotic approach velocity that is used in comparisons with, e.g., the Hill velocity, and this quantity is used, in particular, in the coagulation calculations of Kenyon and Luu (1998).

Figure 3 is a scatter-plot showing the lifetime of trajectories inside the Hill sphere as a function of the ratio $v_{\rm rand}/v_{\rm shear}$. The trajectories that have very long lifetimes inside the Hill sphere - i.e., those that are important in the CAC mechanism - lie, roughly, at the interface between the clearly shear-dominated and the clearly dispersion-dominated regimes. In order to make comparison with other work and the simulations of Kenyon and Luu (1998). asymptotic velocities will be defined as in eq. 11. However, in all simulations the initial conditions are computed using the orbital elements.

In simulations in the planar CHP, Hénon and Petit (1986) and Petit and Hénon (1986) have shown that ranges of impact parameter exist within which encounters inside the Hill sphere are most probable. Lee et al. (2007) have considered a similar problem in the spatial (3D) EHP and find that, similarly, ranges of "optimal" orbital elements exist that are favorable for penetration of the Hill sphere. It should be noted that simply selecting orbital elements within such a range does not guarantee entry into the Hill sphere. In essence an orbital element or, equivalently, a "velocity window" at infinity exists in both the circular and elliptical Hill problems.

The velocity windows in the circular and elliptical Hill problems are shown in Fig. 2 (a) and Fig. 2 (b), respectively. Two observations can be made: (i) The range of

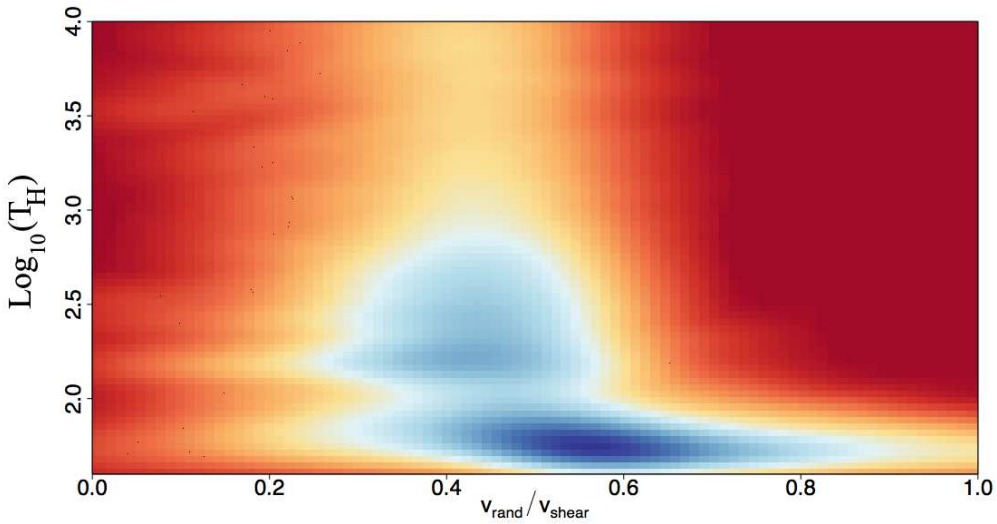


Figure 3.— (colour online) Kernel smoothed scatterplot showing $\log_{10}(T_{\rm Hill})$ where $T_{\rm Hill}$ is the Hill lifetime (in years) in the circular Hill problem as a function of the ratio of the magnitudes of the random and shear asymptotic velocities, $v_{\rm rand}$ and $v_{\rm shear}$, respectively. In Hill units 300 years $\sim 2\pi$; i.e., the Hlll unit of time $\sim$ 50 years at $a_\odot \sim 45$ AU. Scale runs from low [red (online), light grey (print)] to high [blue (online), dark grey (print)]. In this representation smoothed point densities are computed using a kernel density estimator (Gentleman et al., 2006; Carr et al., 1987; Gentleman, 2007). This plot differs from Fig. 1 in that all trajectories that enter the Hill sphere are shown, not just those that end up captured into a binary.

asymptotic random velocities is quite limited in the circular case, being on the order of a few m/s, while (ii) in the elliptical problem the distribution is much wider, which allows for penetration of the Hill sphere by particles that have significantly higher velocities than in the circular case.

## 4 Results

The mass-ratio of any binary that results from intruder scattering is defined using eq. (5), i.e.,

$$m_R = \frac{\alpha_j}{\alpha_k} < 1 \tag{12}$$

where $\alpha_j < \alpha_k$ and $j, k = 1, 2, 3$ are the indices of the two objects that remain bound after intruder scattering.

Two different initial mass distributions were used.

### *4.1 Uniform mass distribution*

As in earlier work, a uniform distribution of masses for $m_1$ and $m_2$ is used, mainly to provide a comparison with the results obtained using a power-law distribution. However,

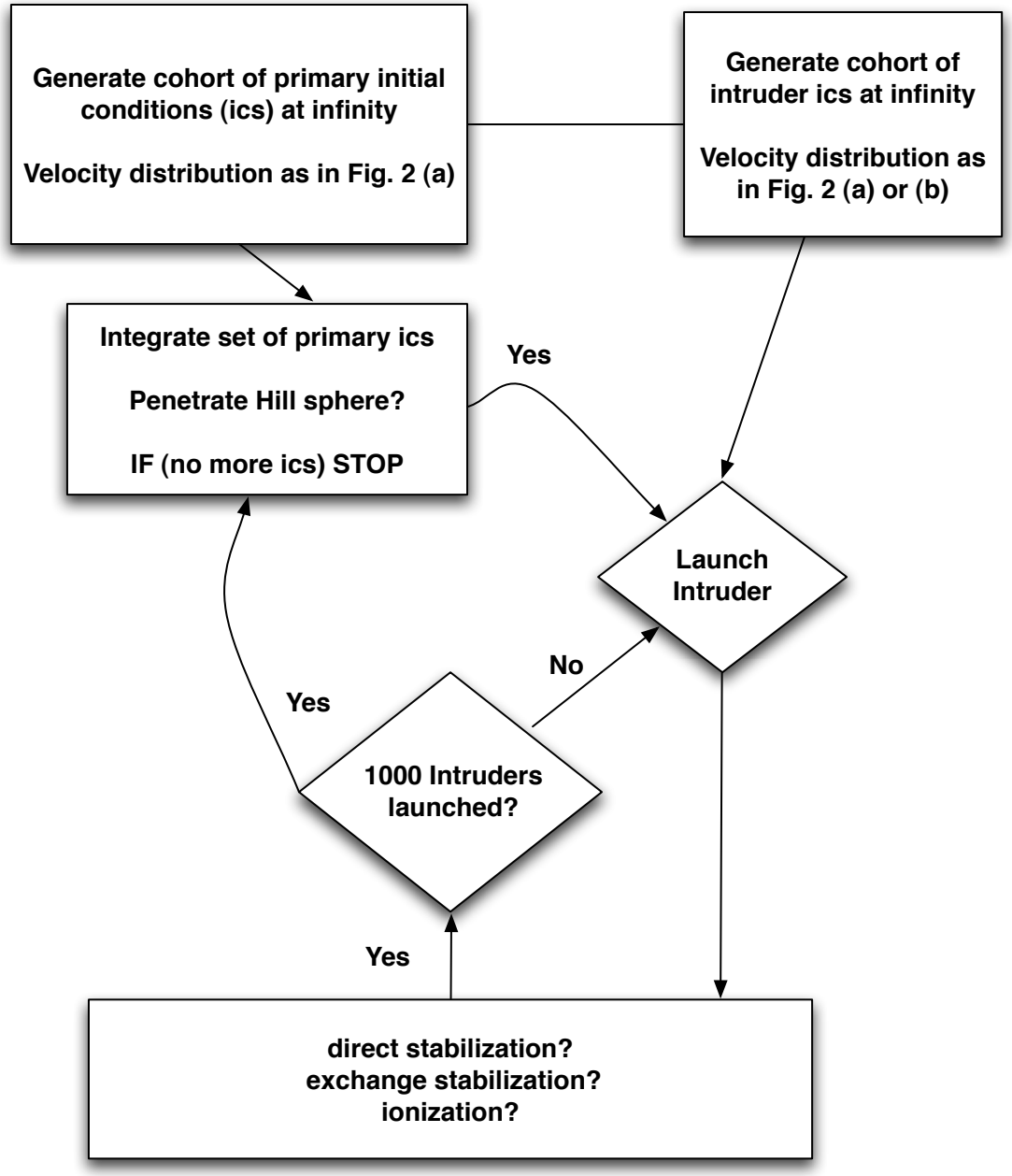


Figure 4.— Flow diagram of the algorithm used in the scattering simulations in the four-body Hill approximation. This plot provides a general overview only. Full details can be found in Lee et al. (2007)

two differences from earlier work exist (Astakhov et al., 2005; Lee et al., 2007): (i) In previous simulations it was assumed that the mass of the intruder did not exceed 50% of the total binary mass. In the current simulations, a uniform mass distribution is used for all three particles, i.e., $\alpha_i \in (0, 1)$ and, (ii) exchange reactions are examined.

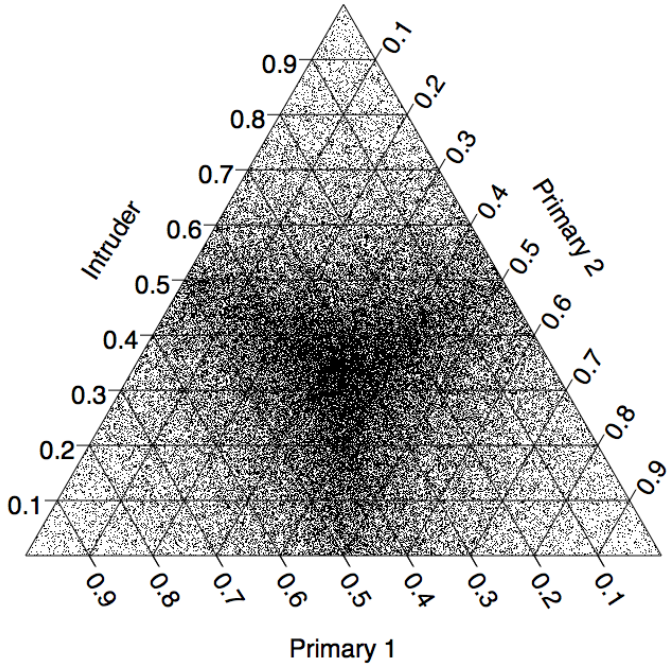


Figure 5.— Ternary scatterplot showing the initial distribution of masses in $\alpha_1, \alpha_2, \alpha_3$ space where "Primary 1" and "Primary 2" refer to $\alpha_1, \alpha_2$, respectively, and $\alpha_3$ corresponds to the intruder.

Because of the relationship in eq. (5), it is possible to display the three relative masses in a ternary scatterplot diagram. A ternary diagram is a triangle, with each of the three apexes representing, in this case, the mass-fraction of one of the three objects, i.e., its $\alpha$-value. The density of points in the scatterplot shows the relative importance of particular sets of $\alpha$-values. Figure 5 shows the initial set of mass-factor ($\alpha$) values used in the simulations. The highest density surrounds the point $\alpha_1 = \alpha_2 = \alpha_3$ because each mass-factor was picked uniformly $\in (0, 1)$ and the three $\alpha$-values sum to unity. Three "legs" radiate symmetrically from this point and correspond to $\alpha_i = \alpha_j$ with $\alpha_k < 1/3$, and $i, j, k = 1, 2, 3$.

Figure 6 shows the corresponding distribution of $\alpha$-values for all scattering events that lead to a stable binary. Although some hint of the structure in the initial distribution of

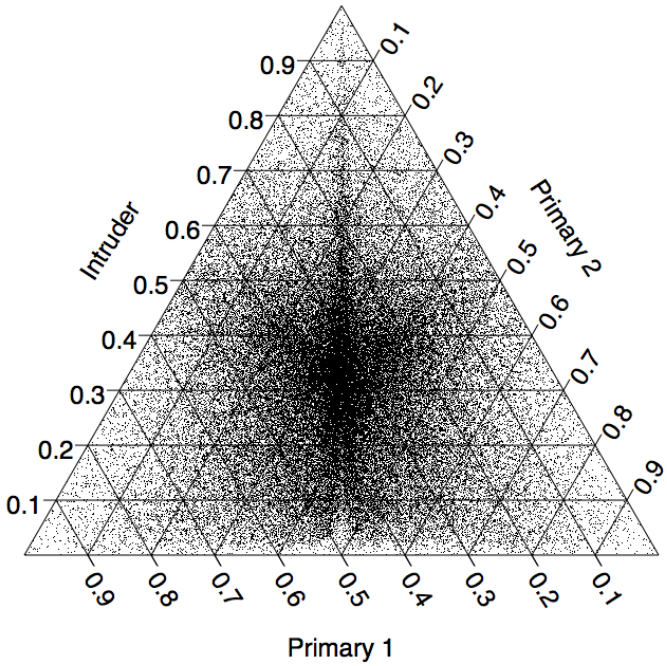


Figure 6.— As for Fig. 5 but for all binaries that end up stabilized, whether that occurred through direct stabilization or exchange. For intruders of all sizes the density is greatest close to the line along which the primaries have equal masses, i.e., $\alpha_1 = \alpha_2$.

masses persists, it is apparent that density along the line $\alpha_1 = \alpha_2$ is significantly enhanced, which reflects the tendency of the CAC model to favor near-symmetric mass binaries.

The corresponding plot when only exchange reactions are included is shown in Fig. 7. It is apparent that exchange reactions also have a significant tendency to produce near-symmetric binaries. Certainly this might be expected from simulations of star-binary scattering, but it should be noted that the present simulations differ from star-binary scattering (Heggie and Hut, 2003) in that the binary is actually quasi-bound and the scattering simulations include the effects of solar tides, i.e., the scattering is essentially four-body rather than three-body. By comparing Fig. 7 with Fig. 6 several conclusions can be drawn:

1. Exchange reactions are most likely when $\alpha_3 > 1/3$, i.e., is larger than one of the primaries.

2. Exchange reactions almost never happen when the primaries have exactly equal masses and $\alpha_3 < 0.4$.

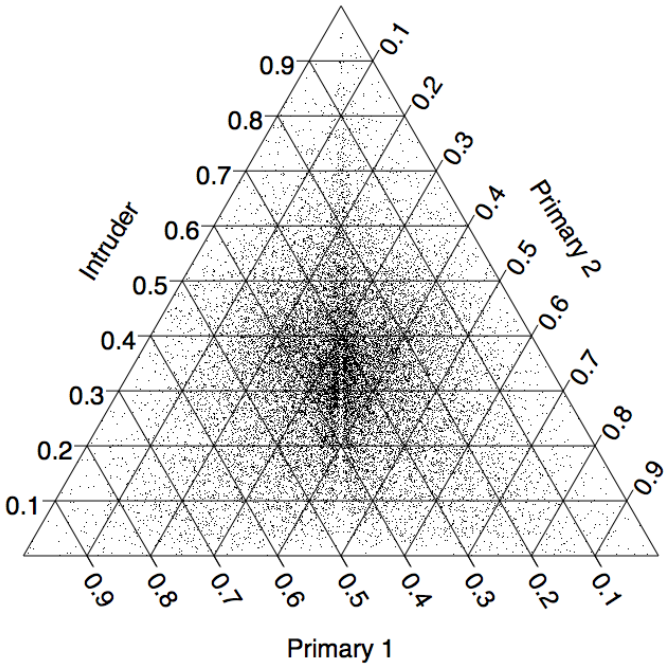


Figure 7.— Same as Fig. 6 except that only exchange reactions are included.

3. If $\alpha_3 > 0.4$, then exchange reactions are somewhat favored if $\alpha_1 = \alpha_2$. In these cases, the intruder is larger than either primary.

4. Surprisingly, even if the intruder is larger than either primary, there remains a tendency to produce a near-symmetric binary even if exchange does not occur. This is evidenced by the strong line of density for $\alpha_1 = \alpha_2$ with $\alpha_3 > 0.4$ in Fig. 6. The corresponding region in Fig. 7 is much less pronounced.

### *4.2 Power-law size distributions*

The computations utilizing a uniform initial distribution of masses demonstrate that the CAC capture mechanism tends to select dynamically for near-symmetric binaries. However, the primordial distribution of TNOs almost certainly followed a power-law size distribution (Kenyon and Luu, 1998, 1999a,b; Kenyon, 2002; Kenyon and Bromley, 2004b,a; Bromley and Kenyon, 2006). Obviously, the nature of the mass (or size) distribution of the particles in the early Kuiper-belt will affect the predictions - and possibly the mechanism - of any KBB formation model. The objective here is not to try to model in any detail the size distribution in the accretional phase of the Kuiper-belt; rather, it

is an attempt to understand how various assumptions about this distribution affect the predictions of the CAC model.

The following differential size-distribution is used

$$n(r) = N/r^4 dr \tag{13}$$

where $r$ is the radius of the TNO, assuming that $r \geq 1$km; $n(r)$ is the number of objects with radius between $r$ and $r + dr$, and $N$ is a normalization factor. This distribution is based on the broken power-law distribution of Kenyon and Bromley (2004b). Clearly this size distribution is skewed very sharply in favor of the smallest objects. Simply drawing primaries and intruders randomly from such a distribution would swamp the simulations with binaries consisting of the very smallest partners. However, coagulation calculations suggest that in $\sim 10 - 12$ Myr bodies having radii in the 100 - 300 km range may have formed in the Kuiper-belt with velocities on the order of a few m/s. According to the results presented by Kenyon and Luu (1998) (Fig. 8) and Kenyon and Luu (1999a) (Fig. 8), the velocities of $\sim 10$ km sized bodies are, as expected, somewhat larger, i.e., on the order of 10 - 15 m/s. Of course, the velocity distributions of 10 km and 100 km sized-bodies may be quite different at different stages of the Kuiper-belt's evolution. Nevertheless, these rather rough estimates of velocities coincide rather well with the velocity windows apparent in Fig. 2.

Assuming that the larger bodies are moving more slowly is equivalent to them moving in less eccentric, less inclined orbits that the smaller bodies. Velocities of a few m/s fall in the velocity window that is necessary for two (relatively) large bodies to penetrate their mutual Hill sphere. On the other hand, smaller, more eccentric bodies will be moving faster, and the velocity distribution in Fig. 2 (b) is more appropriate. Because the time scale for intruder scattering tends to be significantly less than the Hill lifetime of a quasi-bound binary a hybrid approach is used in which (i) the cohort of binary initial conditions is generated in the circular Hill problem, whereas (ii) the cohort of intruder initial conditions is generated in the EHP.

The following algorithm was adopted in simulating intruder scattering using a power-law size distribution for all three bodies.

1. Initial conditions at infinity were selected, as usual, from the cohort of stored initial conditions for the primaries.

2. The relative asymptotic random velocity of the primaries, $v_{\rm rand}$, was computed and stored.

3. The radius of one of the primaries was arbitrarily fixed at 100 km. The radius of the second primary, $r_2$, was drawn randomly from the power-law distribution in eq. (13) with 10 km $\geq r_2 \leq$ 200 km.

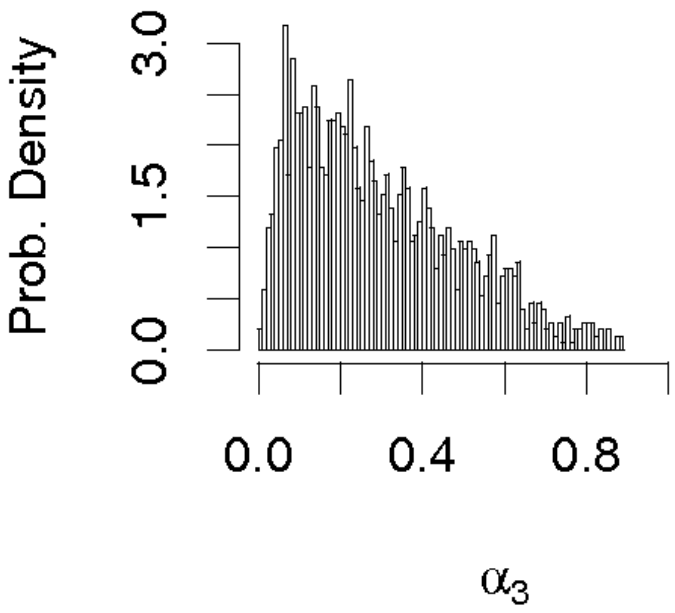


Figure 8.— Distribution of the intruder mass parameter $\alpha_3$ for the simulations using the power law distribution in eq. (13). This is the initial distribution used in the power-law simulations and results from the procedure described in Sec. 13

4. Using the stored value of $v_{\rm rand}$, the velocity of the second primary, $v_2$ was computed.

5. A velocity-radius relationship of the following form was assumed;

$$V(r_2) = V_0 \, \exp\left[-\gamma(r_2 - r_0)^2\right] \tag{14}$$

where $V_0 = 15$ m/s, $r_0 = 10$ km and $\gamma = 0.0005$ km$^{-2}$. This function was chosen to be (very) roughly comparable to interpolating the results in Fig. 8 of Kenyon and Luu (1999a) at $\sim 15$ Myr. However, actual velocity dispersions are not expected to be gaussian, and the choice of fitting function used should not be taken to imply anything about the actual functional form of physical velocity dispersions (Goldreich et al., 2004) - it is a simply a numerical fit.

6. If

$$|v_2| < |v_2'| + \sigma \tag{15}$$

where $\sigma$ is a gaussian random number with a mean of zero and a standard deviation of 4 m/s, then $r_2$ was rejected and a new radius tried. The velocity dispersion of

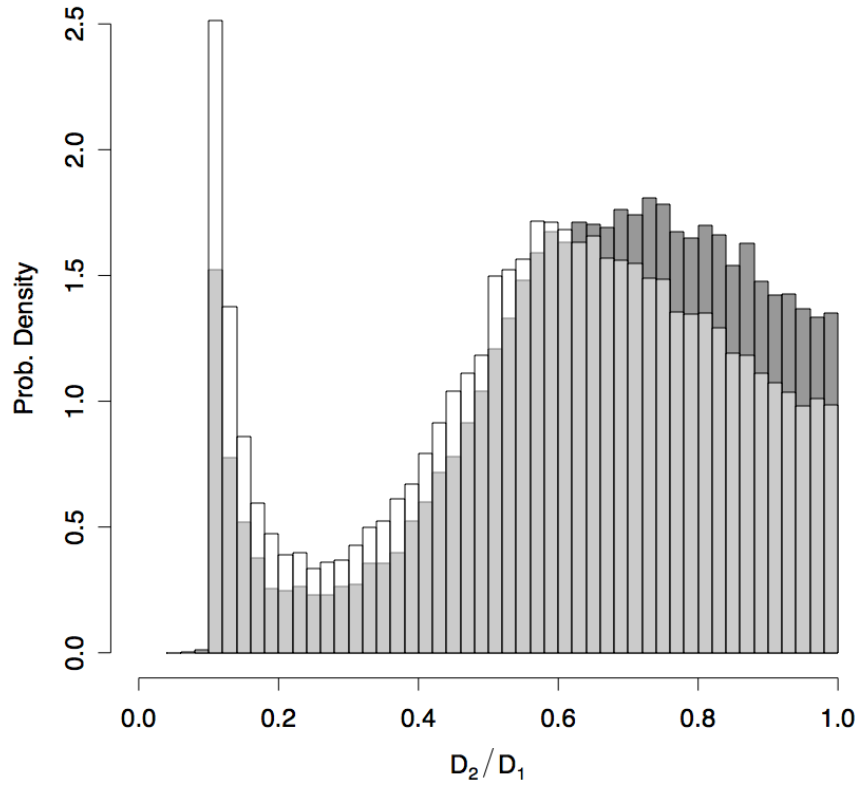


Figure 9.— Results of scattering simulation using a power-law distribution as described in the text. The histograms show the probability density of initial (white) and captured (grey) primary binary diameter ratios $D_2/D_1$ where, by definition, $D_1 \geq D_2$.

4 m/s was chosen somewhat arbitrarily but seems roughly comparable to what is suggested by coagulation calculations. Choosing smaller values for this dispersion tightens the relationship between the radius of a body and its velocity predicted by eq. (14).

7. The same procedure was used to select intruder radii except that the initial conditions were generated in the elliptical Hill three-body problem and, therefore, their velocity distribution is as in Fig. 2 (b).

The idea is to exclude, in some reasonable way, values of $v_2'$ that lie outside the window shown in Fig. 2 (a) for primaries and Fig. 2 (b) for intruders. Obviously, this means unusually fast (small) or slow (large) objects will be rejected. The distribution of intruders chosen in this way and which lead to stabilization is shown in Fig. 8 and is sharply skewed in favor of small intruders. Figure 9 shows the initial and final binary size-ratio distributions - in terms of partner diameters - and there is a clear preference for size-ratios on the order of unity. However, this preference is not solely the result of the dynamical preference for near-symmetric quasi-binaries to be captured, although that is

apparent. In addition, the velocity window that governs entry into the Hill sphere also selects for binary partners of comparable size.

Of course, the results will vary if different assumptions or parameters are used. For example, if a smaller velocity dispersion for the gaussian distribution in eq. (15) is used then the preference for order-unity size ratios can be made more pronounced and the peak at very small size-ratios apparent in Fig. 9 can be made virtually to disappear. Using a larger velocity dispersion has the opposite effect.

## 5 Conclusions

The basic proposition of this article is that capture in the Hill problem requires that two objects in heliocentric Keplerian orbits first enter their mutual Hill sphere. This places constraints on the orbital elements "at infinity" and, more particularly, constraints on the range of velocities that allow entry into the Hill sphere. Equipartition arguments as well as coagulation calculations suggest that a given body's relative velocity will be linked to its mass. This establishes a link between the mass - or size - of a body and its ability to become captured in a binary. Because larger bodies are moving more slowly, two such bodies are more likely to become caught up in the Hill sphere. Stabilization is possible through gravitational scattering with smaller, faster moving intruders.

The main point of the simulations reported here is not to make specific predictions about KBB size-ratios but to investigate how dynamical effects in the CAC model interact with assumptions made about initial mass or size distributions of objects in the early Kuiper-belt. The results suggest that, while dynamical effects tend to select for roughly same-sized binaries, the Hill sphere itself serves to screen out bodies which have relative velocities that do not fall into the window for Hill sphere entry. The actual velocity window itself depends on the heliocentric eccentricities of the particles involved and, therefore, indirectly, on their size.

It is interesting to speculate on the relevance of the CAC mechanism to binary formation in the Asteroid Belt. Main-belt binaries (MBBs) tend to have secondaries that are significantly smaller than their primary, i.e, few MBBs would be considered to be near-symmetric (Noll, 2006). In addition, MBBs generally have much smaller mutual orbit semi-major axes (Noll, 2006). The physical properties of MBBs, and the fact that there appears to be a higher incidence of binaries in collisional families, all point to a collisional formation mechanism (Noll, 2006; Richardson and Walsh, 2006; Durda et al., 2004b; Merline et al., 2004). While this observation does not preclude the operation of CAC as a MBB formation mechanism, the lack of MBBs having KBB-like orbital and compositional properties implies either that CAC didn't function at all in the primordial Asteroid Belt or that any binaries formed by this mechanism have subsequently been destroyed. Given

that the census of main-belt asteroids is compete down to at least diameters of $\sim 20$ km, it is unlikely that the lack of KBB-like MBBs is the result of incomplete surveys of the belt (Chapman, 2005).

The evolution of the main-belt has been the subject of a number of recent studies, and an overview can be found in Petit et al. (2001). The basic idea, first formulated by Wetherill (1992), is that the asteroid belt started out dynamically cold and contained several hundred roughly Mars-sized planetary embryos. These embryos heated up the asteroid belt - thereby explaining the observed dynamical excitation of the belt. After a short period of strong collisional evolution, most planetesimals were ejected from the main belt through gravitational interactions with Jupiter and also between embryos W. F. Bottke et al. (2005). These simulations suggest that the asteroid belt, during this period, can not be well modeled in the three- or four-body Hill approximations since the perturbers - Jupiter and Mars-sized embryos - were all much larger than the diameter, $D \gtrsim 120$ km, sized asteroids which remain in the asteroid belt and that are thought to be relics from primordial times. Because quasi-bound binaries in the CAC scenario are rather delicate Lee et al. (2007) it seems unlikely that any that formed could be stabilized during this period of intense dynamical evolution. For example, the preference for stabilization through small-intruder scattering found in the simulations of Astakhov et al. (2005) and Lee et al. (2007) suggests that the presence of strong gravitational perturbing bodies destabilizes any quasi-bound binaries that might have formed. A more quantitative investigation of these ideas is underway.

For KBBs, a logical next step would be to integrate the CAC model directly with, e.g., coagulation calculations, in order to gain a more quantitative understanding of the interplay between the various dynamical processes that operated in the early Kuiper belt.

## 6 Acknowledgments

This work was supported, in part, by grant No. 0718547 from the National Science Foundation. The author is grateful to the Ministerio de Educación y Ciencia (Spain) for sabbatical support during the academic year 2007-2008.

## References

Agnor, C. B., Hamilton, D. P., 2006. Neptune's capture of its moon Triton in a binary-planet gravitational encounter. Nature 441, 192–194.

Astakhov, S. A., Burbanks, A. D., Wiggins, S., Farrelly, D., 2003. Chaos-assisted capture of irregular moons. Nature 423, 264.

Astakhov, S. A., Farrelly, D., 2004. Capture and escape in the elliptic restricted three-body problem. Mon. Not. R. Astron. Soc. 354, 971–979.

Astakhov, S. A., Lee, E. A., Farrelly, D., 2005. Formation of Kuiper-belt binaries through multiple chaotic scattering encounters with low-mass intruders. Mon. Not. R. Astron. Soc. 360, 401–415.

Barucci, M. A., Fulchignoni, M., Birlan, M., Doressoundiram, A., Romon, J., Boehnhardt, H., 2001. Analysis of trans-Neptunian and Centaur colors: continuous trend or grouping? Astron. Astrophys. 371, 1150–1154.

Bonnell, I. A., 2001. Formation of binary stars. IAU Symposia 200, 23–32.

Bromley, B. C., Kenyon, S. J., 2006. A hybrid $N$-body code for planet formation. AJ 131, 2737–2748.

Brown, M., van Dam, M. A., Bouchez, A. H., Mignant, D. L., Campbell, R. D., Chin, J. C. Y., Conrad, A., Hartman, S. K., Johansson, E. M., Lafon, R. E., Rabinowitz, D. L., Stomski, P. J., Summers, D. M., Trujillo, C. A., Wizinowich, P. L., 2006. Satellites of the largest Kuiper Belt objects. ApJ 639, L43–L46.

Brumberg, V. A., Ivanova, T. V., 1990. Encounters in the Keplerian field: Analytical treatment. Cel. Mech. Dynam. Astron. 49, 133–144.

Burns, J. A., 2004. Double trouble. Nature 427, 494–495.

Canup, R. M., 2005. A giant impact origin of pluto-charon. Science 307, 546–550.

Carr, D. B., Littlefield, R. J., Nicholson, W. L., 1987. Scatterplot matrix techniques for large-$N$. J. Am. Stat. Assoc. 82, 424–436.

Chapman, C. R., 2005. Physical properties of small bodies from Atens to TNOs. In: Lazzaro, D., Ferraz-Mello, S., Fernández, J. A. (Eds.), Asteroids, Comets, and Meteors (IAU S229), Proceedings of the International Astronomical Union Symposia and Colloquia. pp. 3–16.

Chiang, E., Lithwick, Y., Murray-Clay, R., Buie, M., Grundy, W. M., Holman, M., 2006. A brief history of trans-Neptunian space. In: Reipurth, B., et al. (Eds.), Protostars and Protoplanets V.
URL `astro-ph/0601654`

Cruikshank, D. P., 2003. Spectral models of Kuiper Belt objects and Centaurs. Earth, Moon, and Planets 92, 315–330.

Cruikshank, D. P., 2005. Triton, Pluto, Centaurs, and trans-Neptunian bodies. Space Sci. Rev. 116, 421–439.

Cruikshank, D. P., Barucci, M. A., Emery, J. P., Fernández, Y. R., Grundy, W. M., Noll, K. S., Stansberry, J. A., 2006. Physical properties of trans-neptunian objects. In: Reipurth, B., et al. (Eds.), Protostars and Protoplanets V. Ch. (in press).

Durda, D. D., Bottke, W. F., Enke, B. L., Merline, W. J., Asphaug, E., Richardson, D. C., Leinhardt, Z. M., 2004a. The formation of asteroid satellites in large impacts: Results from numerical simulations. Icarus 167, 382–396.

Durda, D. D., W. F. Bottke, J., Enke, B. L., Merline, W. J., Asphaug, E., Richardson, D. C., Leinhardt, Z. M., 2004b. The formation of asteroid satellites in large impacts: results from numerical simulations. Icarus 167, 382–296.

Funato, Y., Makino, J., Hut, P., Kokubo, E., Kinoshita, D., 2004. The formation of Kuiper-belt binaries through exchange reactions. Nature 427, 518–520.

Gentleman, R., 2007. (with Biocore). Geneplotter: Grapics related functions for Bioconductor. R package version 1.12.0
`http://www.bioconductor.org/`
`http://www.ks.uiuc.edu/Research/biocore/`.

Gentleman, R., Hahne, F., Huber, W., 2006. Visualizing genomic data (february 2006). Bioconductor Project Working Papers. Working Paper 10, `http://www.bepress.com/bioconductor/paper10`.

Goldberg, D., Mazeh, T., Latham, D. W., 2003. On the mass-ratio distribution of spectroscopic binaries. AJ 591, 397–405.

Goldreich, P., Lithwick, Y., Sari, R., 2002. Formation of Kuiper-belt binaries by dynamical friction and three-body encounters. Nature 420, 643–646.

Goldreich, P., Lithwick, Y., Sari, R., 2004. Planet formation by coagulation: A focus on Uranus and Neptune. Ann. Rev. Astron. Astrophys. 42, 549–601.

Greenzweig, Y., Lissauer, J., 1990. Accretion rates of protoplanets. Icarus 87, 40–77.

Greenzweig, Y., Lissauer, J., 1992. Accretion rates of protoplanets II: Gaussian distributions of planetesimal velocities. Icarus 100, 440–463.

Heggie, D. C., Hut, P., 2003. The Gravitational Million-Body Problem: A Multidisciplinary Approach to Star Cluster Dynamics. Cambridge University Press.

Hénon, M., Petit, J.-M., 1986. Satellite encounters. Icarus 66, 536–55.

Hills, J. G., 1990. Encounters between single and binary stars - the effect of intruder mass on the maximum impact velocity for which the mean change in binding-energy is positive. AJ 99, 979–982.

Ichtiaroglou, S., 1980. Elliptic Hill's problem: The continuation of periodic orbits. Astron. Astrophys. 92, 139–141.

Iwasaki, K., Ohtsuki, K., 2007. Dynamical behaviour of planetesimals temporarily captured by a planet from heliocentric orbits: basic formulation and the case of low random velocity. Mon. Not. R. Astron. Soc. 377, 1763–1771.

Kenyon, S. J., 2002. Planet formation in the outer Solar System. Pub. Astron. Soc. Pac. 114, 265–283.

Kenyon, S. J., Bromley, B. C., 2004a. Collisional cascades in planetesimal disks II. Embedded planets. AJ 127, 513–550.

Kenyon, S. J., Bromley, B. C., 2004b. The size distribution of Kuiper belt objects. AJ 128, 1916–1926.

Kenyon, S. J., Luu, J. X., 1998. Accretion in the early Kuiper belt. I. Coagulation and velocity evolution. AJ 115, 2136–2160.

Kenyon, S. J., Luu, J. X., 1999a. Accretion in the early Kuiper Belt. II. Fragmentation. AJ 118, 1101–1119.

Kenyon, S. J., Luu, J. X., 1999b. Accretion in the early outer Solar System. ApJ 526, 465–470.

Kern, S. D., Elliot, J. L., 2006. The frequency of binary Kuiper Belt objects. ApJ 643, L57–L60.

Lee, E. A., Astakhov, S. A., Farrelly, D., 2007. Production of trans-Neptunian binaries through chaos-assisted capture. Mon. Not. R. Astron. Soc. 379, 229–246.

Llibre, J., Pinol, C., 1990. On the elliptic restricted three-body problem. Cel. Mech. Dynam. Astron. 48, 319–345.

Lykawa, P. S., Mukai, T., 2005. Higher albedos and size distribution of large transneptunian objects. Planet. Space Sci. 53, 1319–1330.

Margot, J.-L., 2002. Worlds of mutual motion. Nature 416, 694–695.

McKinnon, W. B., Leith, A. C., 1995. Gas drag and the orbital evolution of a captured Triton. Icarus 118, 392–413.

Merline, W. J., Tamblyn, P. M., Nesvorný, D., Durda, D. D., Chapman, C. R., an A. D. Storrs, C. D., Feldman, B., Owen, W. M., Close, L. M., Menard, F., 2004. Discovery of binaries among small asteroids in the Koronis dynamical family using the HST Advanced Camera for Surveys. In: 36th DPS Meeting. p. 46.01.

Merline, W. J., Weidenschilling, S. J., Durda, D. D., Margot, J.-L., Pravec, P., Stoers, A. D., 2002. Asteroids *do* have satellites. In: Bottke, W. F., Cellino, A., Paolicchi, P., Binzel, R. P. (Eds.), Asteroids III. No. pp. 289-312. University of Arizona Press.

Moons, M., Delhaise, F., Depaepe, E., 1988. Elliptical Hill's problem (large and small impact parameters). Cel. Mech. 43, 349–359.

Murray, C. D., Dermott, S. F., 1999. Solar System Dynamics. Cambridge University Press.

Murray-Clay, R. A., Chiang, E. I., 2006. Brownian motion in planetary migration. AJ 651, 1194–1208.

Nakazawa, K., Ida, S., 1988. Hill's approximation xxx. Prog. Theor. Phys. Suppl. 96, 167–174.

Nakazawa, K., Ida, S., Nakagawa, Y., 1989. Collisional xxx. Astron. Astrophys. 220, 293–300.

Noll, K. S., 2003. Transneptunian binaries. Earth, Moon, and Planets 91, 395–407.

Noll, K. S., 2006. Solar System Binaries. In: Lazzaro, D., Ferraz-Mello, S., Fernández, J. A. (Eds.), Asteroids, Comets, and Meteors (IAU S229), Proceedings of the International Astronomical Union Symposia and Colloquia. Cambridge University Press, pp. 301–318.

Noll, K. S., Grundy, W. M., Chiang, E. I., Margot, J.-L., Kern, S. D., 2007. The Kuiper Belt. Space Science Series. University of Arizona Press, (to be published) `http://arxiv.org/abs/astro-ph/0703134`, Ch. Binaries in the Kuiper Belt (to be published).

Noll, K. S., Grundy, W. M., Levison, H. F., Stephens, D. C., 2006. The relative sizes of Kuiper Belt binaries. Bull. Amer. Astron. Soc. 38, 34.03.

Ohtsuki, K., Ida, S., 1990. Runaway planetary growth with collision rate in the Solar gravitational field. Icarus 85, 499–511.

Palacian, J. F., Yanguas, P., Fernandez, S., Nicotra, M. A., 2006. Searching for periodic orbits of the spatial elliptic restricted three-body problem by double averaging. Physica D 213, 15–24.

Person, M. J., Elliot, J. L., Gulbis, A. A. S., Pasachoff, J. M., Babcock, B. A., Souza, S. P., Gangestad, J., 2006. Charon's radius and density from the combined data sets of the 2005 July 11 occultation. AJ 132, 1575–1580.

Petit, J.-M., Hénon, M., 1986. Series expansions for encounter-type solutions of Hill's problem. Cel. Mech. 38, 67–100.

Petit, J.-M., Hénon, M., 1987. Numerical simulation of planetary rings. Astron. Astrophys. 173, 389–404.

Petit, J.-M., Morbidelli, A., Chamber, J., 2001. The primoridal excitation and clearing of the asteroid belt. Icarus 153, 338–347.

Rafikov, R. R., 2003. Dynamical evolution of planetesimals in protoplanetary disks. AJ 126, 2529–2548.

Reinsch, K., Burwitz, V., Festou, M. C., 1994. Albedo maps of Pluto and improved physical parameters of the Pluto-Charon system. Icarus 108, 209–218.

Richardson, D. C., Walsh, K. J., 2006. Binary minor planets. Ann. Rev. Earth and Planet. Sci. 34, 47–81.

Safronov, V. S., 1972. Evolution of the protoplanetary cloud and formation of the Earth and planets. Israel Program for Scientific Translation.

Scheeres, D. J., 1998. The restricted Hill four-body problem with applications to the Earth-Moon-Sun system. Cel. Mech. Dynam. Astron. 70, 75–98.

Shiidsuka, K., Ida, S., 1999. Evolution of the velocity dispersion of self-gravitating particles in disc potentials. Mon. Not. R. Astron. Soc. 307, 737–749.

Simó, C., Stuchi, T. J., 2000. Central stable/unstable manifolds and the destruction of KAM tori in the planar Hill problem. Physica D 140, 1–32.

Stephens, D. C., Noll, K. S., 2006. Detection of six trans-Neptunian binaries with NICMOS: A high fraction of binaries in the cold classical disk. AJ 131, 1142–1148.

Stern, S. A., 1995. Collisional time scales in the Kuiper Disk and their implications. AJ 110, 856–868.

Stern, S. A., 1996. On the collisional environment, accretion time scales, and architecture of the massive, primordial Kuiper belt. AJ 57, 1203–1211.

Stern, S. A., 2002. Implications regarding the energetics of the collisional formation of Kuiper Belt satellites. AJ 124, 2300–2304.

Szebehely, V., 1967. Theory of Orbits: The Restricted Problem of Three Bodies. Academic Press.

Valtonen, M., Mikkola, S., 1991. The few-body problem in astrophysics. Ann. Rev. Astron. Astrophys. 29, 9–29.

Valtonen, M. J., 1998. Mass ratios in multiple star systems. Astron. Astrophys. 334, 169–172.

Veillet, C., Parker, J. W., Griffin, I., Marsden, B., Doressoundiram, A., Buie, M., 2002. The binary Kuiper-belt object 1998 $WW_{31}$. Nature 416, 711–713.

W. F. Bottke, J., Durda, D. D., Nesvorný, D., Jedicke, R., Morbidelli, A., Vokrouhlický, D., Levison, H., 2005. The fossilized size distribution of the main asteroid belt. Icarus 175, 111–140.

Weidenschilling, S. J., 1989. Stirring of a planetesimal swarm: The role of distant encounters. Icarus 80, 179–188.

Weidenschilling, S. J., 2002. On the origin of binary transneptunian objects. Icarus 160, 212–215.

Weidenschilling, S. J., Paolicchi, P., Zappalá, V., 1989. Do asteroids have satellites? In: Binzel, R. P., Gehrels, T., Matthews, M. S. (Eds.), Asteroids II. University of Arizona Press, Tucson, Ariz., pp. 643–658.

Wetherill, G. W., 1992. An alternative model for the formation of the asteroids. Icarus 100, 307–325.

Wetherill, G. W., Cox, L. P., 1984. The range of validity of the 2-body approximation in models of terrestrial planet accumulation. 1. Gravitational perturbations. Icarus 60, 40–55.

Wetherill, G. W., Stewart, G. R., 1989. Accumulation of a swarm of planetesimals. Icarus 77, 330–357.

Wetherill, G. W., Stewart, G. R., 1993. Formation of planetary embryos - effects of fragmentation, low relative velocity, and independent variation of eccentricity and inclination. Icarus 106, 190–209.